Food Hydrocolloids 43 (2015) 8–17

Contents lists available at ScienceDirect

Food Hydrocolloids

journal homepage: www.elsevier.com/locate/foodhyd

Multilayer emulsions as a strategy for linseed oil microencapsulation: Effect of pH and alginate concentration

Silvana A. Fioramonti [a], María J. Martinez [b], Ana M.R. Pilosof [b], Amelia C. Rubiolo [a], Liliana G. Santiago [a,*]

[a] Grupo de Biocoloides, Instituto de Tecnología de Alimentos, Facultad de Ingeniería Química, Universidad Nacional del Litoral, Santa Fe, Argentina
[b] Departamento de Industrias, Facultad de Ciencias Exactas y Naturales, Universidad de Buenos Aires, Buenos Aires, Argentina

ARTICLE INFO

Article history:
Received 26 February 2014
Accepted 17 April 2014
Available online 14 May 2014

Keywords:
Emulsion stability
Sodium alginate
Whey protein isolate
Flocculation
Creaming
Layer-by-layer deposition

ABSTRACT

The influence of pH (4–7) and sodium alginate (SA) concentration (0.125–0.25 wt%) on the properties of linseed oil-in-water emulsions stabilized by a whey protein isolate (WPI) was investigated. Droplet size, droplet charge, creaming stability and optical microscopy measurements as well as determination of non-adsorbed biopolymers at the oil–water interface were made. At pH 6 and 7, anionic alginate did not adsorb onto the surfaces of WPI-coated droplets due to strong electrostatic repulsion between biopolymers. Remaining SA molecules in the continuous phase induce emulsion destabilization by depletion flocculation, with the formation of floc chains that, after a period of latency, promoted phase separation with high creaming indexes. Both the delay time and the cream layer thickness increased when increasing SA concentration. At pH 5, ζ-potential measurements demonstrate deposition of SA onto WPI interfacial membrane to form a bilayer around oil droplets. Besides, no droplet aggregation was observed and emulsions were stable to creaming after one-week storage. At pH 4, 0.125 wt% SA emulsions were prone to extensive droplet aggregation probably enhanced by bridging flocculation, exhibiting a gel-like microstructure of interconnected flocs, which then promoted phase separation. However, when increasing initial SA concentration in these systems, the degree of droplet aggregation decreased. These results suggest that the best conditions to produce stable emulsions as encapsulation matrices for the delivery of high polyunsaturated fatty acid oils would be 0.25 wt% SA pH 5.

1. Introduction

Numerous studies have shown that dietary intake of ω-3 polyunsaturated fatty acids (PUFAs) could provide several health benefits. These benefits include decreased risk of cardiovascular disease, protection against cognitive decline during aging as well as improved neuronal growth and brain development in early infancy (Hibbeln, Nieminen, Blasbalg, Riggs, & Lands, 2006; Innis, 2007; Uauy & Dangour, 2006). Fish oil has been chosen as the preferential source of long chain ω-3 essential fatty acids, mainly for its eicosapentaenoic (EPA, C20:5) and docosahexaenoic (DHA, C22:6) acid content. Nevertheless, linseed oil is a good vegetable alternative ω-3 source in nature, since it contains high levels of α-linoleic acid (ALA), which makes about 55–60% of total fatty acids (Gallardo et al., 2013). Although linseed oil has been widely used in the industry for paint and varnish manufacturing, it has not yet been exploited for the production of functional foods. The main reason is that there are some limitations regarding the development of ω-3 fortified products since PUFAs are extremely sensitive to lipid oxidation, leading to the formation of off-flavors and potentially toxic compounds that would alter nutritional quality of food. Therefore, microencapsulation arises as an adequate technique to overcome these issues (Garg, Wood, Singh, & Moughan, 2006; Klinkesorn, Sophanodora, Chinachoti, Decker, & McClements, 2005). Oil-in-water (O/W) conventional single-layer emulsions have been used as delivery systems for the encapsulation of PUFAs and incorporated into dairy products (milk, ice cream, yogurts) and burgers (Chee et al., 2005; Lee, Faustman, Djordjevic, Faraji, & Decker, 2006; McClements & Decker, 2000). Nevertheless, this type of emulsions are thermodynamically unstable when exposed to environmental stresses, such as heating, cooling, freezing, drying or extreme pH values (McClements, Decker, & Weiss, 2007). There is an emerging technology which consists in the designing of multilayer emulsions where the lipid droplets are coated by nanolaminated self-

* Corresponding author. Tel.: +54 342 4571252x2602.
E-mail addresses: lsanti@fiq.unl.edu.ar, lgsantiago2006@yahoo.com.ar (L. G. Santiago).

http://dx.doi.org/10.1016/j.foodhyd.2014.04.026
0268-005X/

assembled biopolymer layers, formed by electrostatic interactions (McClements et al., 2007). The advantage of this method is that interfacial layers of greater thickness can be obtained around the oil droplet, providing not only an increased emulsion stability against environmental stresses but also better protection for the bioactive agent entrapped within the core (Sagalowicz & Leser, 2010). Besides, physicochemical properties of the interfacial film can be carefully designed by manipulating the system composition and the emulsifying conditions (biopolymer type and concentration, pH, ionic strength, etc.) (Guzey & McClements, 2006). Proteins and polysaccharides are natural polymers that are widely used as functional ingredients in the food industry (McClements, 2006). In particular, milk whey proteins are very versatile because they have not only high nutritional values but also great technological qualities, including the ability to stabilize foams and emulsions (Dalgleish, Senaratne, & Francois, 1997; Molina Ortiz, Puppo, & Wagner, 2004). Due to their amphiphilic properties, these proteins can quickly adsorb onto the oil–water interface, creating an elastic high-resistant surface layer around the oil droplet (Taherian, Britten, Sabik, & Fustier, 2011). An opposite charged polysaccharide can be added to this primary emulsion to produce a secondary emulsion, by inducing the electrostatic deposition of the polysaccharide onto the protein surface to form an outer coating. This can be achieved by manipulating the charge density of both biopolymers through pH variation (Guzey & McClements, 2006).

To address a successful microencapsulation of PUFAs, a stable emulsion has to be obtained. However, emulsions can undergo a variety of physical instabilities, including creaming, flocculation and coalescence. Creaming involves a gravitational separation due to the upward movement of the droplets resulting from the difference between the dispersed and the continuous phase density, whereas flocculation and coalescence are both types of droplet aggregation (McClements, 1999). One of the most important factors to prevent droplet aggregation is to control biopolymer concentration in the aqueous phase, such that there is enough biopolymer to completely saturate the oil–water interface, but not too much as this could promote depletion flocculation (Guzey & McClements, 2006). A number of investigations have been carried out to produce multilayer emulsions and examine the factors that influence their stability (Khalloufi, Alexander, Goff, & Corredig, 2008; Klinkesorn et al., 2005; Perrechil & Cunha, 2013). In general, all these works have been made on the basis of particle size, ζ-potential and rheology measurements. However, few works concern about the determination of non-adsorbed biopolymers remaining in the continuous phase and how this would affect emulsion stability. Besides, to the knowledge of the authors, there are no studies about emulsions stabilized by multilayered membranes composed of sodium alginate and whey protein isolate.

In this context, the objective of this work was to evaluate the influence of pH and sodium alginate concentration on the overall stability of oil-in-water emulsions, so as to determine the best conditions to encapsulate linseed oil.

1.1. Theoretical aspects

Global stability of emulsions could be discussed in terms of interdroplet pair potentials that involve both attractive and repulsive interactions between two emulsion droplets coming close together. Theoretical models often rely on certain simplifying assumptions to facilitate mathematical treatment in order to derive tractable expressions that describe the behavior of ideal systems. Although these assumptions are not always fulfilled in real systems, an understanding of the various types of interactions which act between emulsion droplets represents a powerful tool for interpreting data and for systematically accounting for the effects of different factors in many food matrices (McClements, 1999).

If we consider a system which consists of two spherical emulsion droplets of radius r, at a surface-to-surface separation h, the total interaction potential (U_{TOTAL}) between them will be the resultant of individual contributions of different attractive and repulsive interaction potentials:

$$U_{TOTAL}(h) = U_{attractive}(h) + U_{repulsive}(h) \quad (1)$$

Most relevant individual interaction potentials between emulsion droplets will be briefly described.

1.1.1. Van der Waals interactions

The Van der Waals interdroplet pair potential (U_{WDV}) between two emulsion droplets of equal radius r, separated by a surface-to-surface distance h is given by the following expression:

$$U_{VDW}(h) = \frac{-A}{6}\left[\frac{2r^2}{h^2+4rh} + \frac{2r^2}{h^2+4rh+4r^2} + \ln\frac{h^2+4rh}{h^2+4rh+4r^2}\right] \quad (2)$$

where A is the Hamaker constant (McClements, 1999). Assuming that the droplets are separated by short distances ($h \ll r$), then the above equation simplifies to:

$$U_{VDW}(h) = \frac{-Ar}{12h} \quad (3)$$

Van der Waals interdroplet pair potential is always attractive and promotes droplet aggregation.

1.1.2. Electrostatic interactions

Electrostatic interdroplet pair potential is given by:

$$U_{ELECTROSTATIC}(h) = 2\pi\varepsilon_0\varepsilon_R r\zeta^2 \ln(1+\exp[-\kappa h]) \quad (4)$$

where ε_0 is the dielectric constant of vacuum, ε_R is the relative dielectric constant of the solution surrounding the droplets, ζ is the electrical potential at the shear plane (known as zeta potential), and κ is the inverse of the *Debye screening length* (Radford & Dickinson, 2004). The latter parameter is given by:

$$\kappa^{-1} = \frac{[\varepsilon kT(1-\phi_{oil})]^{1/2}}{2e^2 I N_A} \quad (5)$$

where k is the Boltzmann constant, T is the temperature, ϕ_{oil} is the oil volumen fraction, e is the charge on an electron, I is the ionic strength and N_A is the Avogadro's number.

Electrostatic interactions are repulsive if droplets have similar charges and decrease at large droplet separations. At short distances, the electrostatic repulsion is usually weaker than the Van der Waals attraction so, under these conditions, the droplets will tend to aggregate (McClements, 1999).

1.1.3. Steric interactions

Polymeric steric interactions arise when emulsion droplets get so close together that the emulsifier layers overlap. This type of potential can be divided into two contributions:

$$U_{STERIC}(h) = U_{mix}(h) + U_{elastic}(h) \quad (6)$$

Mixing contribution (U_{mix}) is entirely due to the intermingling of the polymer chains when two droplets come close together, without the interface layer being compressed. McClements (1999)

proposes the following equation to describe this interaction potential:

$$U_{\mathrm{mix}}(h) = 4\pi rkTm^2 N_A \frac{\bar{v}_P^2}{V_S}(½ - \chi)\left(1 - ½\frac{h}{\delta}\right)^2 \quad (7)$$

where m is the mass of polymer chains per unit area, δ is the thickness of the adsorbed layer, χ is the Flory-Huggins parameter, $\bar{v}_P$ is the partial specific volume of the polymer chains, and V_S is the molar volume of the solvent. In a good solvent ($\chi < 0.5$), such as water, the increment in concentration of the polymer chains in the interpenetration zone is thermodynamically unfavorable as it reduces the number of polymer-solvent contacts, leading to a repulsive interaction between the droplets.

Elastic contribution (U_{elastic}) is entirely due to the compression of the interfacial membrane that arises when two droplets approach, without considering any interpenetration of the polymer molecules. Jackel (1964) proposed an empirical model to assess this type of interaction:

$$U_{\mathrm{elastic}}(h) = 0.77E(½\delta - ½h)^{5/2}(r + \delta) \quad h < \delta \quad (8)$$

$$U_{\mathrm{elastic}}(h) = 0 \quad h \geq \delta \quad (9)$$

where E is the elastic modulus of the adsorbed layer. Compression of the interfacial layer involves a decrease in the configurational entropy of the adsorbed molecules. This phenomenon is energetically unfavorable, so this type of interaction is always repulsive. Besides, it has to be taken into account that at short distances, the polymeric steric repulsion is stronger than the Van der Waals attraction (McClements, 1999).

1.1.4. Depletion interactions

Depletion interdroplet pair potential appears in emulsions where droplets are surrounded by colloidal nonadsorbing molecules, which remain in the continuous phase. When the separation between two droplets is small compared to their size ($h \ll r$) and approximately equivalent to the hydrodynamic radius of the colloidal particle, an exclusion region in the middle of the droplets is generated. The concentration of colloidal particles in this depletion zone tends to zero, whereas in the surrounding continuous phase it has a finite value. This creates an osmotic potential difference that promotes the movement of solvent molecules from the exclusion region into the bulk liquid, leading to the aggregation of the droplets (McClements, 1999). This interdroplet pair potential is given by:

$$U_{\mathrm{DEPLETION}}(h) = \frac{-2}{3}\pi r^3 P_{\mathrm{OSM}}\left[2\left(1 + \frac{r_c}{r}\right)^3 + \left(1 + \frac{h}{2r}\right)^3 - 3\left(1 + \frac{r_c}{r}\right)^2\left(1 + \frac{h}{2r}\right)\right] \quad (10)$$

where P_{OSM} is the osmotic pressure arising from the exclusion of the colloidal particles and r_c is the radius of the colloidal particles. The osmotic pressure difference is given by:

$$P_{\mathrm{OSM}} = \frac{CRT}{M}\left(1 + \frac{N_A C v}{2M}\right) \quad (11)$$

where C, M and v are the concentration, molecular weight, and volume of the colloidal particles and R is the universal gas constant. As can be seen, this interaction potential is always attractive and increases when increasing concentration of colloidal particles in the continuous phase.

1.1.5. Total interaction potential

Considering the above described potentials as the most significant regarding our experimental systems, it can be assumed that the overall interdroplet potential is the sum of the various attractive and repulsive contributions:

$$U_{\mathrm{TOTAL}}(h) = U_{\mathrm{VDW}}(h) + U_{\mathrm{ELECTROSTATIC}}(h) + U_{\mathrm{STERIC}}(h) + U_{\mathrm{DEPLETION}}(h) \quad (12)$$

2. Materials and methods

2.1. Materials

Milk whey protein isolate (WPI) was provided by Davisco Food International, Inc. (Minnesota, USA) and its composition (% w/w) was: 96.18% protein ($N \times 6.38$) (dry basis), fat 0.20%, ash 1.90%, 5.57% moisture, 1.72% others. A commercial sample of low density sodium alginate (SA) was provided by Cargill (Buenos Aires, Argentina) (PM 135 kDa). As stated by the manufacturer the composition of this alginate was: carbohydrate 63%, moisture 14%, ash 23% (Na^+ 9300 mg/100 g and K^+ 800 mg/100 g). Linseed oil was obtained from Sigma Aldrich (St. Louis, MO) and it was used as supplied, without previous purification (density: 0.93 g/mL, refractive index: 1.48). All reagents were analytical grade.

2.2. Emulsion preparation

Stock dispersions of 2 wt% WPI were prepared using Milli-Q ultrapure water and were stirred for 2 h. Sodium alginate (SA) was dispersed in Milli-Q ultrapure water and stirred at 70 °C for 35 min to promote solubilization. The pH value of all dispersions was adjusted to 7.0 with HCl and NaOH (0.1 mol l^{-1}) and then dispersions were stored at 4 °C overnight. Primary emulsions were made by blending 20 wt% oil phase with 80 wt% aqueous WPI solution using a high-speed blender (Waring Blender, Connecticut, USA) during 2 min at the highest velocity, followed by a sonication step (75% AMP, 150 s) performed by a 20 KHz ultrasonic probe with 13 mm diameter tip (Sonics & Materials, Connecticut, USA). These microemulsions were then diluted by adding sodium alginate (SA) dispersions and adjusting the pH to different values (7, 6, 5, 4) to form secondary emulsions, with the following final composition: 10 wt% oil, 1 wt% WPI, and 0.125–0.25 wt% SA. All emulsions were analyzed just after being prepared.

2.3. Droplet size determination

Droplet size of emulsions was measured by static light scattering using a laser diffraction Mastersizer 2000 device with a Hydro 2000MU as a dispersion unit (Malvern Instruments, Worcestershire, Inglaterra). The pump speed was settled between 900 and 1500 rpm. The refractive index of both the dispersed (1.48) and the continuous phase (1.33) were used. Droplet size is reported as the volume-mean diameter (D_{43}):

$$D_{43} = \frac{\sum n_i d_i^4}{\sum n_i d_i^3} \quad (13)$$

where n_i is the number of droplets of diameter d_i (Camino, Carrera Sanchez, Rodríguez Patino, & Pilosof, 2012). To determine the

distribution width of droplet sizes, the span (or polydispersity index) was also reported as follows:

$$\text{Span} = \frac{(D_{0.9} - D_{0.1})}{D_{0.5}} \quad (14)$$

where 90, 10 and 50% of the oil volumen in the emulsions is contained in droplets with diameters below or equal to $D_{0.9}$, $D_{0.1}$ and $D_{0.5}$ respectively. Droplet sizes are reported as the average of ten readings made on each sample.

2.4. ζ-potential measurements

ζ-potential of emulsion droplets was determined by dynamic laser light scattering using a Zetasizer Nano-ZS instrument (Malvern Instruments, Worcestershire, England) provided with a He–Ne laser beam (633 nm). The emulsion was diluted 1/1000 with the corresponding solution prior to analysis to avoid multiple scattering effects and was then injected into the cuvette. The ζ-potential was determined by measuring the direction and velocity of droplet movement in a well-defined electric field. These measurements are reported as the average and standard deviation of five determinations per sample.

2.5. Determination of coalescence and free biopolymer

After 24 h storage at room temperature, emulsions were centrifuged at 20,000 g and 10 °C for 30 min (Heal Force, Neofuge 18R, China). First, the total oil released above the upper cream phase was determined gravimetrically. The separated oil percentage was calculated as follows:

$$\text{Coalescence}(\%) = \left(\frac{m_1}{m_2}\right) \cdot 100 \quad (15)$$

where m_1 is the mass of the separated oil after centrifugation and m_2 is the mass of total oil added to the emulsion (Santiago, Carrara, & González, 2005). The serum fraction was also recovered to determine the concentration of (i) the non-adsorbed protein to the oil–water interface, by UV absorbance at 280 nm (Aitken & Learmonth, 1996, p. 3–6), and (ii) the remaining polysaccharide via the phenol-sulfuric method described by Dubois, Gilles, Hamilton Rebers, and Smith (1956).

2.6. Emulsion stability

The destabilization of the emulsions was evaluated using a Turbiscan TMA 2000 (Formulaction, Toulouse, France). The sample was placed in a cylindrical glass cell, and scanned from the bottom to the top with a light source ($\lambda = 850$ nm). Simultaneously, two synchronized optical sensors respectively recorded light transmitted through the sample (180° from the incident light), and light backscattered by the sample (45° from the incident radiation). These data are represented in curves of Transmittance and/or Backscattering (%) as a function of the sample height (mm). The scans are repeated over time, each time providing a single curve, and at the end of the experiment, all curves are superimposed on the same graph to show the overall destabilization of the system. This complete analysis mode enables the detection of both the migration phenomena and the variation of average particle size. To better visualize the changes undergone in the systems, it is convenient to work in the reference mode (Δ% BS or Δ% T), which substracts the first curve ($t = 0$) from the subsequent ones (Fig. 1) in order to see the variations of profiles related to the initial state. The profiles recorded for each sample were then analyzed using the proper software, from which we obtained (i) the creaming index, expressed as:

$$\text{Creaming index}(\%) = \frac{H_S}{H_T} \cdot 100 \quad (16)$$

where H_S is the height of the serum layer, and H_T is the height of the total emulsion (Gu, Decker, & McClements, 2005), as a parameter of the global emulsion destabilization after 7 days of storage at room temperature, (ii) the average Δ%BS variation measured the middle zone of the profiles (25–35 mm) as a function of time, which is related to the variation of droplet size (Fig. 1), and (iii) the delay time, which corresponds to the period of latency preceding the phase separation.

2.7. Optical microscopy

Emulsions were properly stirred before analysis to ensure sample homogeneity. A drop of fresh emulsion was then placed between a microscope slide and a cover-slip and observed on a conventional optical microscope at a magnification of 40X (Leica Microsystems, Wetzlar, Germany).

2.8. Statistical analysis

All assays were measured at least in duplicate. Averages and standard deviations were calculated from these measurements.

3. Results and discussion

3.1. Effect of pH and SA concentration on droplet size distribution and droplet charge of emulsions

First, droplet size distributions of emulsions as a function of pH (7–4) at different SA concentrations (0.125–0.25 wt%) were obtained (Fig. 2). The values of D_{43} and polydispersity for each system are presented in Table 1. It can be seen that emulsions prepared at pH 5, 6 and 7, for both SA concentrations, showed a monomodal distribution with D_{43} values in the range of 1–2.5 μm. However, size distributions of emulsions evaluated at pH 4 were more polydisperse and, unlike the other systems, presented a second peak corresponding to droplets sizes around 100 μm (Fig. 2). This phenomenon can be also evidenced by D_{43} and span values, which were much higher than those corresponding to pH 5, 6 and 7. Since the technique used to determine droplet sizes requires performing a previous dilution of the sample to fit in the measuring range, the behavior observed in emulsions at pH 4 might be due to a droplet aggregation phenomenon that was not reversible upon dilution. Besides, at this pH, the systems prepared with 0.125 wt% SA showed a higher polydispersity and a higher D_{43} than those prepared with

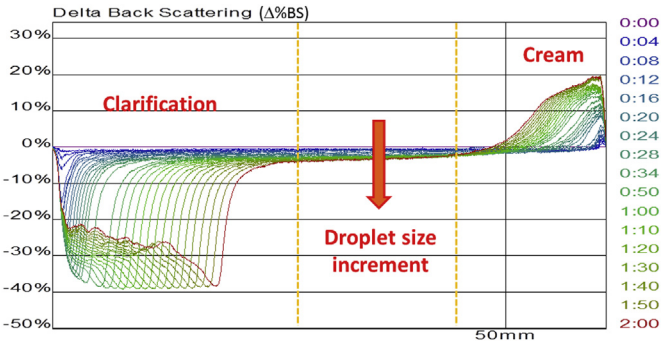

Fig. 1. Illustrative Turbiscan Backscattering profile of the destabilization of a 10 wt% oil 1 wt% WPI 0.125 wt% SA pH 7 emulsion over time. Each curve corresponds to a single time measurement.

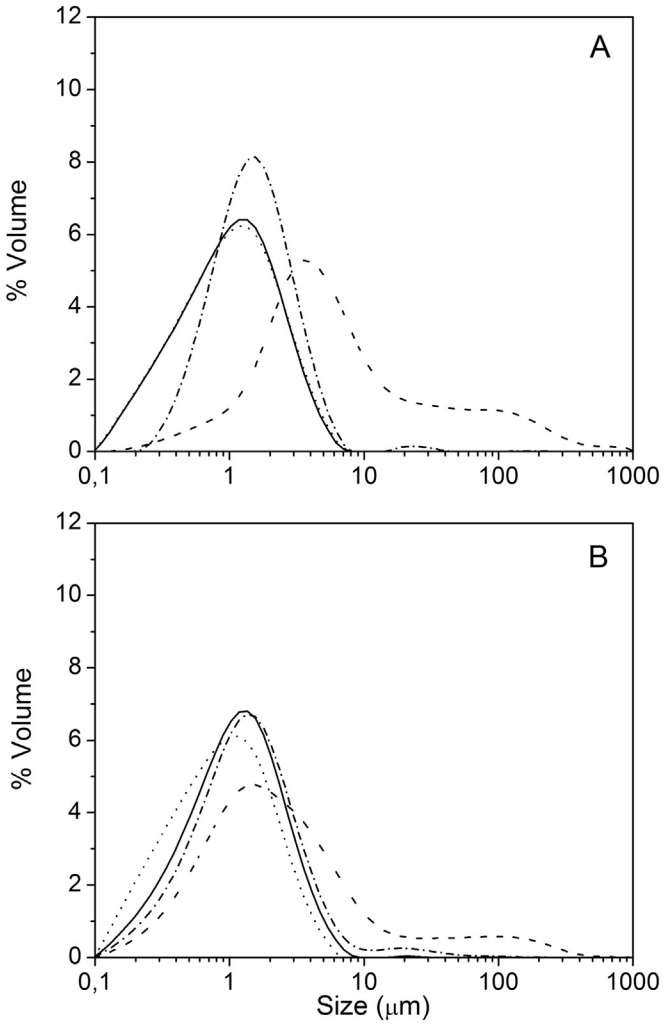

Fig. 2. Influence of pH (····· 7, —— 6, -·- 5, – – 4) on droplet size distribution of 10 wt% oil 1 wt% WPI containing 0.125 wt% SA (A) or 0.25 wt% SA (B).

0.25 wt% SA, suggesting that larger droplet aggregates might have been formed in this conditions.

Secondly, zeta potential measurements were performed to evaluate the electrostatic deposition of the polysaccharide onto the protein interfacial film surrounding the droplets (Fig. 3). It was observed that, in the absence of SA, the surface charge of primary emulsion droplets was −70 and −11 mV at pH 7 and 5, respectively. This variation in the zeta potential with the decrease of pH could be attributed to the net charge of WPI molecules adsorbed onto the droplets' surface, becoming less negative at pH values near the protein isoelectric point (pI = 5.2–4.7) (Pongsawatmanit, Harnsilawat, & McClements, 2006).

In contrast, ζ-potential of secondary emulsions varied from −70 to −30 mV as pH decreased from 7 to 4. According to literature, the magnitude of electrostatic interactions between protein and polysaccharide molecules depends on both the density and the distribution of the charges along each biopolymer at a specific pH (Gu et al., 2005). At pH 7, the net surface charge of the droplets of primary and secondary emulsions was the same for all systems (−70 mV). These results could be explained taking into account that both WPI and SA molecules have a net negative charge at neutral pH, and they are mutually excluded by electrostatic repulsion (Rodríguez Patino & Pilosof, 2011; Weinbreck, 2004). Thus, given the limited interaction between biopolymers under these conditions, SA molecules would not adsorb onto the protein interface and the net surface charge of droplets would be governed by WPI aminoacidic residues. However, as pH falls towards the protein pI, the net negative charge of WPI gradually decreases and approaches to zero. Under these conditions, positively charged "patches" exposed on the protein surface could interact with negatively charged groups present in the polysaccharide chains (De Kruif, Weinbreck, & de Vries, 2004; Jones & McClements, 2011). Fig. 3 shows that, at pH 5, the net surface charge of secondary emulsion droplets (−51 and −54 mV) was much higher than that for primary emulsions (−11 mV), thus suggesting the adsorption of SA onto the WPI interfacial film. At pH 4, a similar behavior was observed. Under these conditions, as the WPI is below its pI, it would exhibit a net positive charge density (Pongsawatmanit et al., 2006). Nevertheless, secondary emulsion droplets showed a negative ζ-potential value, a bit smaller than that observed for pH 5, indicating the adsorption of the SA onto WPI interfacial monolayer to form a bilayer around the droplets. The lower ζ-potential observed at pH 4 could be related to greater charge neutralization between the adsorbed biopolymers, presumably due to an increased number of positive patches exposed on the protein surface. This greater charge neutralization could also induce droplets to come closer together, promoting the formation of aggregated flocs of larger sizes (Fig. 2). Furthermore, secondary emulsions prepared with 0.125 wt% SA at pH 4 and 5, showed a ζ-potential value slightly less than that observed in the respective systems containing 0.25 wt% AS (Fig. 3). Providing that in these conditions the electrostatic interaction between SA and the adsorbed WPI was demonstrated, this phenomenon could be attributed to an increased charge neutralization in emulsions containing 0.125 wt% SA, promoted by a higher WPI:SA ratio (8:1) (Fioramonti, Perez, Aríngoli, Rubiolo, & Santiago, 2014).

3.2. *Effect of pH and SA concentration on biopolymer adsorption at the oil–water interface*

The ability of proteins to form an interfacial film that is resistant to rupture plays an important role in stabilizing emulsion droplets against flocculation and coalescence during long-term storage (McClements, 2004). However, the non-adsorbed biopolymer molecules that remain in the continuous phase might cause (i) formation of protein–polysaccharide complexes which, depending on pH, could precipitate to produce coacervates (Fioramonti et al., 2014) and/or (ii) destabilization of the systems through depletion flocculation mechanisms (Dickinson, 2010). Hence, the importance of the non-adsorbed polymers determination. Fig. 4 shows the concentration of non-adsorbed both WPI and SA, remaining in the aqueous phase, as a function of pH. On the one hand, in Fig. 4A it can be seen that, for both initial SA concentrations, soluble WPI decreases as pH falls. Particularly, WPI concentration in the aqueous phase remained constant at pH 6 and 7, representing approximately 20% of the initial protein concentration. Besides, no differences were observed between emulsions prepared with different initial SA concentrations. However, at pH 5, soluble WPI concentration slightly began to decrease, reaching the minimum value at pH 4. On the other hand, Fig. 4B shows soluble SA concentrations in the aqueous phase, where a behavior similar to that previously described was observed. At higher pH values, SA concentration remained almost constant and close to initial concentration, whereas at lower pH values, SA concentration began to decrease. It should be added that all emulsions made at pH 4 and 5 exhibited the formation of a precipitate at the bottom of the test tubes after centrifugation, with the exception of 0.25 wt% SA pH 5 emulsions (data not shown). In the first place, the amount of WPI adsorbed at the oil–water interface could be directly related to the emulsion preparation technique and to the total energy provided to

Table 1
Volume-mean diameter D_{43}, polydispersity index (span) and delay times of 10 wt% oil 1 wt% WPI emulsions, prepared at different pH and SA concentrations.

Emulsion	D_{43} (μm)	Span	Delay time t_D (h)
0.125% SA pH 7	1.32 ± 0.01	2.47 ± 0.01	0.28
0.125% SA pH 6	1.31 ± 0.02	2.39 ± 0.15	0.26
0.125% SA pH 5	2.03 ± 0.26	1.90 ± 0.03	Stable
0.125% SA pH 4	29.29 ± 2.13	15.42 ± 0.16	2
0.25% SA pH 7	1.17 ± 0.00	2.50 ± 0.02	$24 > t_D > 2$
0.25% SA pH 6	1.47 ± 0.02	2.31 ± 0.05	$24 > t_D > 2$
0.25% SA pH 5	2.41 ± 0.07	2.56 ± 0.06	Stable
0.25% SA pH 4	13.66 ± 2.09	10.79 ± 1.36	Stable

the system to create interfacial area (Jafari, Assadpoor, He, & Bhandari, 2008). Furthermore, since at pH 6 and 7 there was limited interaction between biopolymers due to electrostatic repulsive forces, soluble SA concentration remained close to the initial concentration in the aqueous phase, and soluble WPI concentration stayed constant. Nevertheless, as pH moved towards WPI pI, the protein surface could have gradually expose positively charged "patches" which started to interact with negatively charged polysaccharide molecules, as discussed above. Therefore, two phenomena might be occurring simultaneously: (i) electrostatic deposition of SA onto WPI interfacial film to form a bilayer around the oil droplet and (ii) soluble complexes formation between WPI and SA molecules remaining in the continuous phase. Both phenomena would be more favored at pH 4, since at this pH value there is a higher density of positive charges present on WPI surface, which would promote stronger interactions with SA molecules. In addition, these latter WPI–SA complexes present in the aqueous phase would tend to precipitate when subjected to high centrifugal forces – such as the ones we used to determine soluble biopolymers – with the subsequent formation of a coacervate at the bottom of the test tube (De Kruif et al., 2004; Fioramonti et al., 2014). This would contribute to a decrease in WPI and SA concentration in the continuous phase.

A phenomenon of particular interest occurred in SA 0.25 wt% pH 5 systems, where no coacervate formation was observed after centrifugation, thus suggesting the decrease of SA concentration in the aqueous phase (Fig. 4B) could be exclusively due to the electrostatic deposition of SA molecules onto WPI interfacial membrane surrounding the oil droplets to form a second biopolymer layer.

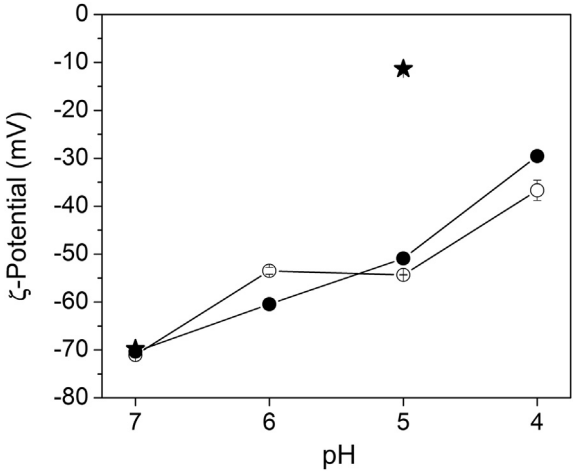

Fig. 3. Effect of pH on zeta potential of 10 wt% oil 1 wt% WPI emulsions containing 0 wt% SA (★), 0.125 wt% SA (●) and 0.25 wt% SA (○).

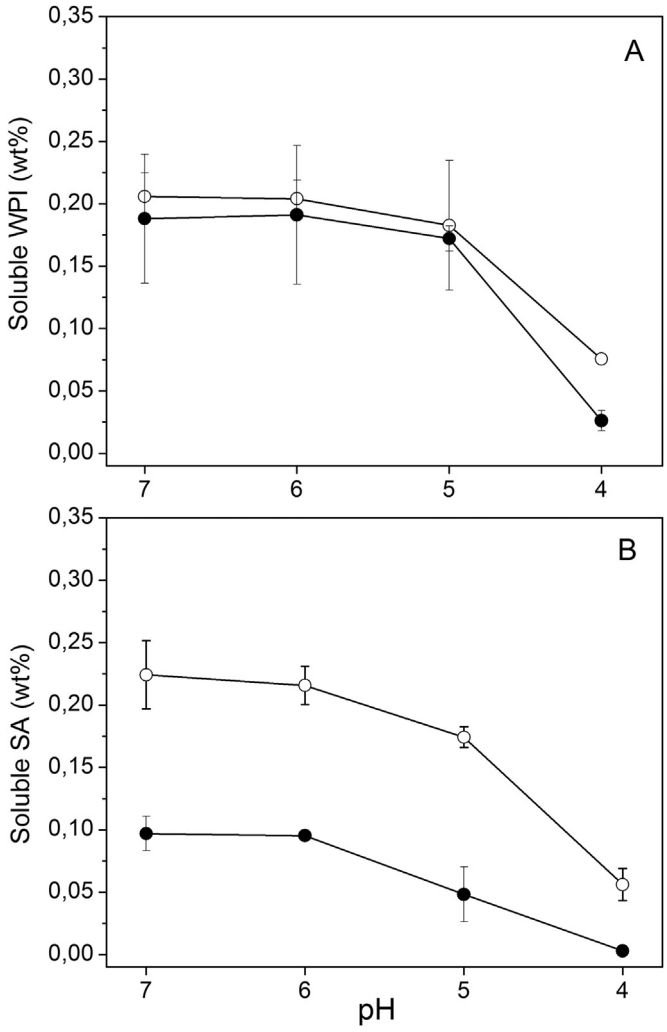

Fig. 4. Effect of pH on free soluble WPI (A) and SA (B) in the aqueous phase of 10 wt% oil 1 wt% WPI emulsions containing 0.125 wt% SA (●) or 0.25 wt% SA (O).

In addition, 0.125 wt% SA pH 4 emulsions showed a higher reduction of protein content in the aqueous phase (Fig. 4A) than their 0.25 wt% SA counterparts, which could be due to the formation of a greater amount of coacervate after centrifugation. This behavior might be explained considering initial WPI:SA ratios when preparing emulsions. Since 0.125 wt% SA emulsions had a higher WPI:SA ratio (8:1) than 0.25 wt% SA ones (4:1), the decrease in pH in the former systems would have promoted a greater charge neutralization between biopolymers forming WPI–SA complexes in the continuous phase, which would have favored the formation of greater amounts of coacervate. These results are consistent with those obtained in previous work (Fioramonti et al., 2014). It must be highlighted that centrifugation of emulsions did not produced "oiling off" from the cream layer in any case, emphasizing the excellent functional properties of WPI to form a sufficiently elastic interfacial film with great mechanical resistant to coalescence.

3.3. *Effect of pH an SA concentration on emulsion stability*

3.3.1. *Flocculation/coalescence stability*

Emulsion stability against flocculation/coalescence was evaluated by analyzing backscattering profiles (Δ%BS) obtained from Turbiscan. Fig. 5 shows the evolution of the average value of Δ%BS (calculated in the middle zone of profiles, as shown in Fig. 1) as

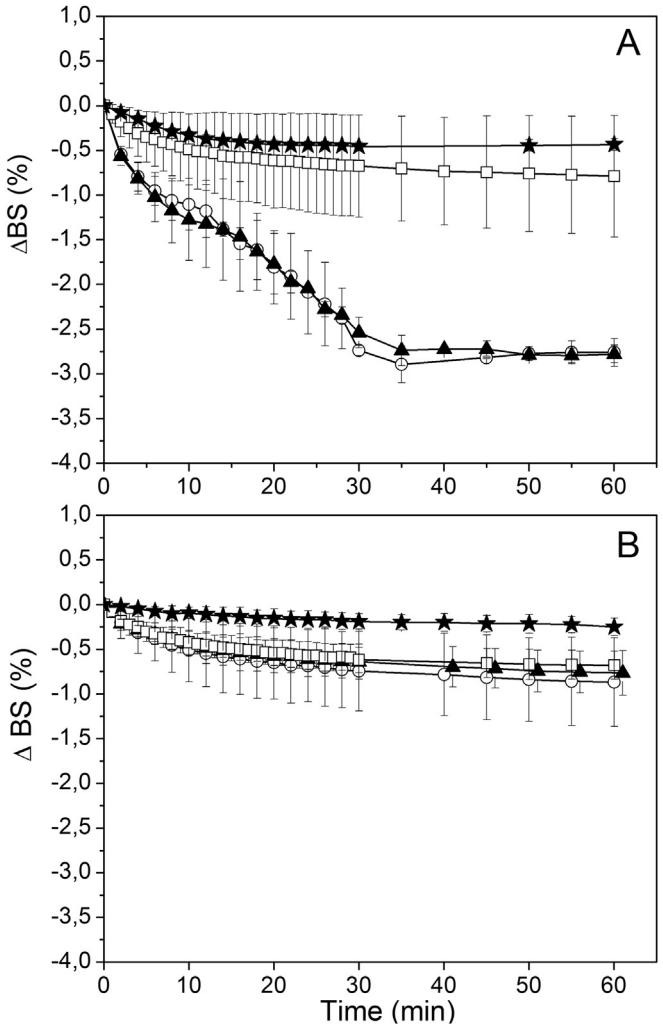

Fig. 5. Effect of pH (○ 7, ▲ 6, □ 5, ★4) on the ΔBackscattering profiles of 10 wt% oil 1 wt% WPI emulsions containing 0.125 wt% SA (A) or 0.25 wt% SA (B), as a measure of droplet size variation. Mean values for each system were determined from the middle zone of the tube (25 mm–35 mm height).

function of time, as a measure of droplet size variation promoted by flocculation/coalescence processes during the first hour of analysis. The intensity of backscattered light is related to the number of droplets located at a specific height of the emulsion. In our case, a reduction of Δ%BS represents a decrease in the number of droplets, caused by an increment on particle size, either by flocculation or coalescence. Coalescence comprises an irreversible process because it involves the rupture of the interfacial film resulting in the fusion of two or more droplets to form a larger droplet. Whereas flocculation is a process that leads droplets to come together to form aggregates, but retaining their individual integrity as the interfacial membrane is conserved (McClements, 1999). These two phenomena lead to an increase in droplet sizes, which can be detected by the Turbiscan. However, the instrument is not able to discriminate to which of these destabilization mechanisms droplet size increment corresponds. As shown in Fig. 5A, 0.125 wt% SA systems at pH 6 and 7 exhibited a marked decrease of Δ% BS, indicating an increase in droplet size; while at pH 4 and 5 the Δ% BS remained almost constant, suggesting droplet size did not change. Meanwhile, emulsions prepared with 0.25 wt% SA (Fig. 5B) presented a similar behavior at pH 4 and 5. But at pH 6 and 7, the decrease in Δ% BS was not as notable as the one shown in their corresponding 0.125 wt% SA counterparts, indicating only a slight variation in droplet size. Since we have demonstrated the absence of coalescence after emulsion centrifugation in previous results, droplet size increment shown in Fig. 5 could be attributed to flocculation. As shown in Fig. 6, emulsions prepared at pH 6 and 7 exhibited a particular microstructure, where formation of flocculated droplet chains can be clearly distinguished, at both SA concentrations. As discussed above, in these conditions, both WPI and SA possess a net negative charge density and there is limited interaction between them. Several authors suggest that the presence of nonadsorbing colloidal particles in the continuous phase of an emulsion would promote an increase in the attractive forces between the droplets due to an osmotic process associated with the exclusion of the colloids from a narrow region surrounding the droplets (Guzey & McClements, 2006; McClements, 1999; Radford & Dickinson, 2004). This phenomenon is called depletion flocculation and can accelerate emulsion destabilization through formation of droplet aggregates or "flocs" with greater sizes than individual droplets. If we consider theoretical interdroplet pair potentials, the flocculated chains observed at pH 7 for both SA concentrations (Fig. 6), might be indicating that U_{TOTAL} (Eq. (12)) between emulsion droplets was strongly attractive. Under these conditions, non-adsorbed SA molecules remaining in the continuous phase (Figs. 3 and 4) could

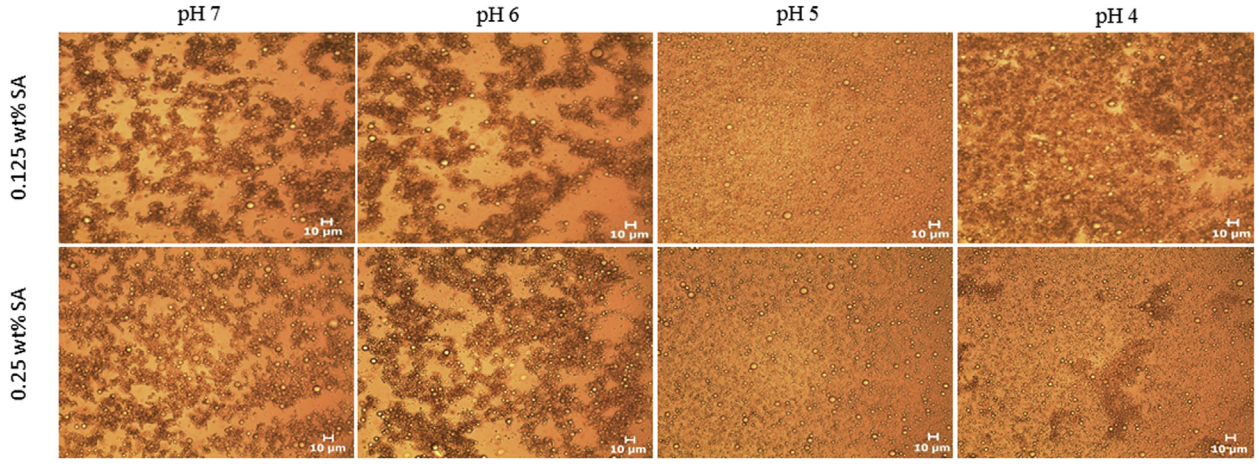

Fig. 6. Influence of pH and SA concentration on microstructure of 10 wt% oil 1 wt% WPI emulsions. The scale bar corresponds to 10 µm.

have generated an attractive $U_{DEPLETION}$ (Eq. (10)) between the droplets. Consequently, the osmotic pressure difference, which is the main driving force of this potential, would have favor the movement of solvent molecules from the depletion zone into the bulk liquid, thus promoting droplet aggregation. Besides, given that at short distances attractive U_{VDW} (Eq. (3)) contribution would prevail over repulsive $U_{ELECTROSTATIC}$ (Eq. (4)) contribution, a resulting attractive U_{TOTAL} would be the responsible for the aggregated state of the droplets. However, we should also take into account the repulsive U_{STERIC} contribution (Eq. (6)), which dominates U_{VDW} at very short distances ($h < \delta$), thus preserving the interfacial membrane integrity and avoiding droplet coalescence. The behavior observed in emulsions at pH 6, for both SA concentrations, could be analyzed in a similar way. In this case, the repulsive $U_{ELECTROSTATIC}$ (Eq. (4)) contribution would be smaller than the corresponding to pH 7, due to the lower ζ-potential value observed in these systems (Fig. 3). In addition, there would still be an attractive $U_{DEPLETION}$ (Eq. (10)), since the concentration of non-adsorbed biopolymers was similar to that observed at pH 7 (Fig. 4). Therefore, U_{TOTAL} (Eq. (12)) would remain being attractive and emulsion droplets would be flocculated. Many authors consider that higher concentrations of nonadsorbing colloidal particles would promote a greater degree of depletion flocculation (McClements, 2000; Perrechil & Cunha, 2013). Nevertheless, emulsions prepared with 0.25 wt% SA could present a slower initial flocculation rate than their 0.125 wt% SA counterparts (Fig. 5), presumably because of the viscosity increment in the continuous phase when increasing polysaccharide concentration (Manoj, Fillery-Travis, Watson, Hibbered, & Robins, 1998).

On the other hand, emulsions prepared at pH 5 exhibited unflocculated individual droplets, at both SA concentrations (Fig. 6). Unlike other systems, stability of these emulsions seemed to be governed by the existence of a net repulsive U_{TOTAL} (Eq. (12)) between the droplets. Although the repulsive $U_{ELECTROSTATIC}$ (Eq. (4)) contribution in these emulsions would be even smaller than that observed at pH 6 and 7, due to a lower ζ-potential value (Fig. 3), there would still be another stabilizing force that maintains droplets apart from each other. Previous results have demonstrated the adsorption of the polysaccharide onto the protein interfacial monolayer to form a multilayer around the oil droplet at pH 5. So, this phenomenon would lead to (i) a decrease of SA concentration in the continuous phase (Fig. 4), that would probably reduce the magnitude of the attractive $U_{DEPLETION}$ (Eq. 10) and (ii) an increase in the interfacial layer thickness (δ), which would promote a greater repulsive U_{STERIC} (Eq. (6)), through both U_{mix} (Eq. (7)) and $U_{elastic}$ (Eq. (8)) contributions. Moreover, it has to be remembered that at short distances steric repulsion is stronger than the Van der Waals attraction (McClements, 1999). Hence, repulsive contributions would prevail above attractive potentials, thereby generating a repulsive U_{TOTAL} which would prevent droplet aggregation.

Surprisingly, at pH 4, emulsions showed different microscopic structures depending on SA initial concentrations (Fig. 6). On the one hand, 0.125 wt% SA systems presented completely flocculated emulsion droplets, forming a dense network (that differs from the floc chains observed at pH 6 and 7), which would denote a resultant attractive U_{TOTAL} (Eq. (12)) between the droplets. In these systems, repulsive $U_{ELECTROSTATIC}$ (Eq. (4)) would be smaller than that at pH 5, mainly because of the greater charge neutralization between the assembled biopolymers at the interfacial membrane (Fig. 3). Fig. 4 shows that almost no polysaccharide was left in the aqueous phase. However, as centrifugation of these systems yielded large amounts of coacervate, former WPI–SA complexes produced in the continuous phase, could have probably induced an attractive $U_{DEPLETION}$ between the droplets, since they might have acted as nonadsorbing colloidal particles (McClements, 1999). Besides, if available SA soluble molecules were not enough to completely saturate the protein interface, then (i) δ would be smaller than that observed at pH 5, decreasing the repulsive U_{STERIC} contribution (Eq. (6)), and (ii) a "bridging" flocculation phenomenon would be promoted, where a single molecule of polysaccharide may adsorb to the surface of two droplets (Dickinson, 2011; Gu et al., 2005). This latter effect would force droplets to come closer and the attractive U_{VDW} (Eq. (3)) contribution would be relevant in these conditions. Consequently, the sum of all these contributions would result in an attractive U_{TOTAL} between the droplets. On the other hand, emulsions containing 0.25 wt% SA at pH 4 showed a few isolated flocs coexisting with a population of non-flocculated droplets (Fig. 6). This lower degree of droplet aggregation produced by increasing initial SA concentration, could be attributed to a greater number of SA molecules adsorbed onto the protein interface, thus promoting an increased repulsion, both electrostatic (Fig. 3) and steric, between the droplets. In this system, the analysis of the individual contributions of different interdroplet pair potentials would be more complex because of the coexistence of both aggregated flocs and unflocculated droplets.

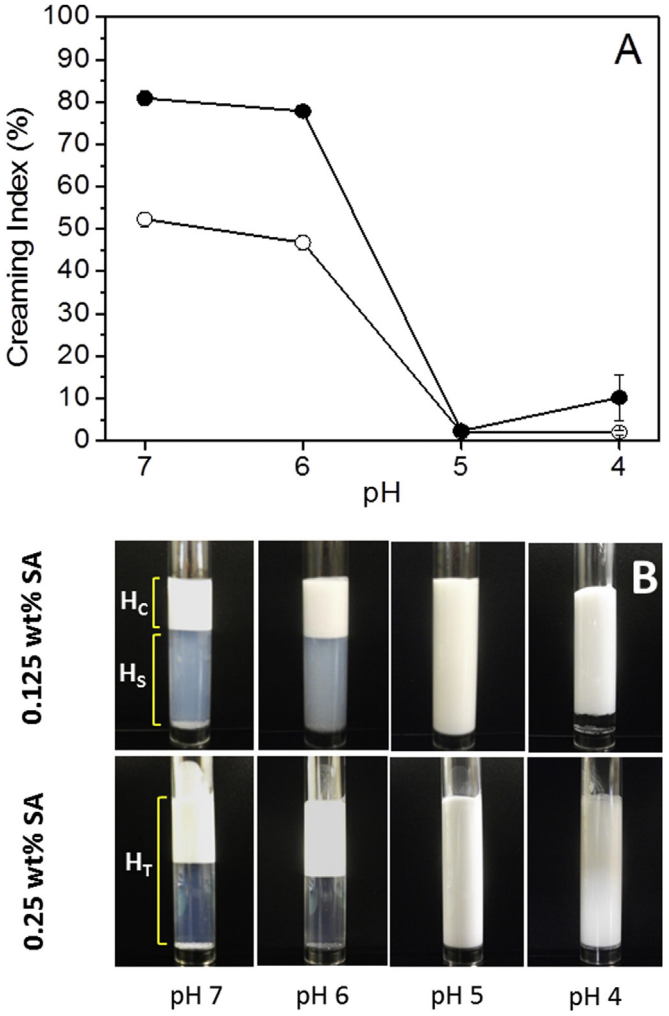

Fig. 7. (A) Effect of SA concentration (● 0.125 wt%, ○ 0.25 wt%) and pH on the creaming index of 10 wt% oil 1 wt% WPI emulsions, after 1 week storage. (B) Visual appearance of 10 wt% oil 1 wt% WPI oil-in-water emulsions containing 0.125 wt% or 0.25 wt% SA at different pH values, after 1 week storage. H_T: height of the total emulsion, H_S: height of the serum layer, H_C: thickness of the cream layer.

3.3.2. Creaming stability

A creaming index was determined for each emulsion after 7 days of analysis, as a parameter of long-term global stability. These values are represented in Fig. 7A, where it can be noted that emulsions prepared at pH 6 and 7 were the most unstable to creaming, regardless of the initial SA concentration; while those prepared at pH 5 were the most stable ones. Delay times, which correspond to a "latency" period prior to the onset of phase separation (Lizarraga, Pan, Añón, & Santiago, 2008) are presented in Table 1. This parameter is related to the flocculation degree of emulsions and several authors suggest that delay time increases when increasing concentration of non-adsorbed polymers in the continuous phase (Lizarraga et al., 2008; Parker, Gunning, & Robins, 1995; Santiago et al., 2002).

First, emulsions prepared with 0.125 wt% SA at pH 6 and 7 exhibited higher creaming indexes (Fig. 7A) and lower delay times (Table 1) than those prepared with 0.25 wt% SA. As shown in Fig. 7B, systems prepared with 0.25 wt% SA exhibited a visually clear serum, whereas those prepared with 0.125 wt% SA presented a high turbidity in the serum phase, which was visually cloudy. These results are consistent with those reported by Manoj et al. (1998), where a similar behavior was observed when increasing polysaccharide concentration in the continuous phase of hexadecane oil-in-water emulsions. The lower concentration of SA (0.125 wt%) might not have been enough to fully flocculate the droplets at pH 6 and 7. In these conditions, emulsions would contain two phases, a flocculated phase in coexistence with unflocculated droplets. The latter would be responsible for the turbidity observed in the serum phase, as individual droplets would cream slower than flocculated ones. Therefore, the cloudy aspect of the serum could be due to the presence of these suspended individual droplets. On the contrary, emulsions prepared with the highest SA concentration (0.25 wt%) would be completely flocculated. In these systems, the formation of a space-spanning flocculated structure might occur, due to the high degree of flocculation. One model proposed by Manoj et al. (1998), is that the flocs could form a porous network which slowly rearranges to produce channels through which continuous phase could flow. In this case, the delay time could be related to the time for the droplets to rearrange to that channeled structure. Since the increase in SA concentration might contribute to an increment in the viscosity of the continuous phase, both the rate of flocculation and the diffusion of the droplets through the channels could be reduced, thus increasing the delay time of these systems (Table 1). However, after this period of latency, the sudden collapse of such a network would promote the rapid creaming of flocs, resulting in a clear serum layer due to the absence of individual residual droplets. The thickness of cream layers (H_C) also seemed to be related to initial SA concentration of systems prepared at pH 6 and 7 (Fig. 7B). The higher the SA initial concentration, the greater the cream layer thickness. So, an increment in polysaccharide concentration would probably increase the compressive strength of the flocculated structure, yielding more expanded creams than lower SA concentrations.

Secondly, emulsions prepared at pH 5 (at both SA concentrations) were the most stable ones and no phase separation was evidenced after 7 days of analysis. The same happened with the system prepared with 0.25 wt% SA at pH 4. However, the emulsion prepared at pH 4 with 0.125 wt% SA showed a little creaming index, with a transparent serum layer, as indicative of complete flocculation (Fig. 7). These results are consistent with the existence of a highly flocculated network previously observed in the micrographs (Fig. 6). At pH 4, the main obstacle to the creaming could have been the formation of a gel-like structure of interconnected flocs (Meller & Stavans, 1996). The collapse of this structure, after the delay time, would have led to phase separation.

4. Conclusions

The stability of multilayer emulsions was dependent on both pH and initial SA concentration. At pH 6 and 7, both WPI and SA molecules presented a net negative charge density so electrostatic deposition of the polysaccharide around the protein membrane surrounding the oil droplets did not occur. Destabilization of these systems was evidenced through depletion flocculation mechanisms, with the formation of floc chains that promoted phase separation. Both the delay time and the thickness of the cream layer increased when increasing SA concentration in the continuous phase. The most stable emulsions were obtained at pH 5 and 0.25 wt% SA, mainly due to the adsorption of the polysaccharide onto the protein interfacial membrane through attractive electrostatic interactions between negatively charged SA molecules and positively charged "patches" exposed on WPI surface. In these systems, neither phase separation nor coacervate formation was observed. Finally, emulsions at pH 4 presented coacervate formation. Those prepared with the lowest SA concentration showed phase separation and exhibited a gel-like microstructure of interconnected flocs forming a network, which would have been promoted by the greater charge neutralization between biopolymers and, possibly, by "bridging" flocculation. The degree of flocculation of these systems decreased when increasing initial SA concentration. In this context, we can conclude that emulsions prepared at pH 5 with 0.25 wt% SA presented the best stability. Therefore, we propose these conditions to prepare encapsulation matrices for delivery of oils with high levels of polyunsaturated fatty acids. Nevertheless, additional studies should be carried out in the future to evaluate the oxidative stability of these bioactive agents over different storage conditions.

Acknowledgment

This research was supported by the following projects: CAI+D PI 2011 (50120110100171LI) and CATT 2011 (Scale-up project), both from Universidad Nacional del Litoral (UNL, Argentina). Authors would like to thank Carolina Arzeni for her advice and kind collaboration on droplet size and zeta-potential determinations. We also want to acknowledge the National Scientific and Technical Research Council of Argentina (CONICET) for the postgraduate fellowship awarded to Silvana Fioramonti.

References

Aitken, A., & Learmonth, M. (1996). *The protein protocols handbook, part I*.

Camino, N. A., Carrera Sanchez, C., Rodríguez Patino, J. M., & Pilosof, A. M. R. (2012). Hydroxypropylmethylcellulose-β-lactoglobulin mixtures at the oil-water interface. Bulk, interfacial and emulsification behavior as affected by pH. *Food Hydrocolloids, 27*, 464–474.

Chee, C. P., Gallaher, J. J., Djordjevic, D., Faraji, H., McClements, D. J., Decker, E. A., et al. (2005). Chemical and sensory analysis of strawberry flavoured yogurt supplemented with an algae oil emulsion. *Journal of Dairy Research, 72*(3), 311–316.

Dalgleish, D. G., Senaratne, V., & Francois, S. (1997). Interactions between β-lactalbumin and α-lactoglobulin in the early stages of heat denaturation. *Journal of Agricultural and Food Chemistry, 45*, 3459–3464.

De Kruif, C. G., Weinbreck, F., & de Vries, R. (2004). Complex coacervation of proteins and anionic polysaccharides. *Current Opinion in Colloid & Interface Science, 9*, 340–349.

Dickinson, E. (2010). Flocculation of protein-stabilized oil-in-water emulsions. *Colloids and Surfaces B: Biointerfaces, 81*, 130–140.

Dickinson, E. (2011). Mixed biopolymers at interfaces: competitive adsorption and multilayer structures. *Food Hydrocolloids, 25*, 1966–1983.

Dubois, M., Gilles, K. A., Hamilton, J. K., Rebers, P. A., & Smith, F. (1956). Colorimetric method for determination of sugars and related substances. *Analytical Chemistry, 28*(3), 350–356.

Fioramonti, S. A., Perez, A. A., Aríngoli, E. E., Rubiolo, A. C., & Santiago, L. G. (2014). Design and characterization of soluble biopolymer complexes produced by electrostatic self-assembly of a whey protein isolate and sodium alginate. *Food Hydrocolloids, 35*, 129–136.

Gallardo, G., Guida, L., Martinez, V., López, M. C., Bernhardt, D., Blasco, R., et al. (2013). Microencapsulation of linseed oil by spray drying for functional food application. *Food Research International, 52*, 473–482.
Garg, M. L., Wood, L. G., Singh, H., & Moughan, P. J. (2006). Means of delivering recommended levels of long-chain omega-3 polyunsaturated fatty acids in human diets. *Journal of Food Science, 71*(5), 66–71.
Gu, Y. S., Decker, E. A., & McClements, D. J. (2005). Influence of pH and carrageenan type on properties of β-lactoglobulin stabilized oil-in-water emulsions. *Food Hydrocolloids, 19*, 83–91.
Guzey, D., & McClements, D. J. (2006). Formation, stability and properties of multilayer emulsions for application in the food industry. *Advances in Colloid and Interface Science, 128–130*, 227–248.
Hibbeln, J. R., Nieminen, L. R. G., Blasbalg, T. L., Riggs, J. A., & Lands, W. E. M. (2006). Healthy intakes of omega-3 and omega-6 fatty acids: estimations considering worldwide diversity. *American Journal of Clinical Nutrition, 83*(6), 1483S–1493S.
Innis, S. (2007). Dietary ω-3 fatty acids and brain development. *The Journal of Nutrition, 137*, 855–859.
Jackel, V. K. (1964). Über die Funktionen des Schutzkolloids. *Kolloid-Zeitschrift und Zeitschrift für Polymere, 197*, 143–151.
Jafari, S. M., Assadpoor, E., He, Y., & Bhandari, B. (2008). Re-coalescence of emulsion droplets during high-energy emulsification. *Food Hydrocolloids, 22*, 1191–1202.
Jones, O. G., & McClements, D. J. (2011). Recent progress in biopolymer nanoparticle and microparticle formation by heat-treating electrostatic protein-polysaccharide complexes. *Advances in Colloid and Interface Science, 167*, 49–62.
Khalloufi, S., Alexander, M., Goff, H. D., & Corredig, M. (2008). Physicochemical properties of whey protein isolate stabilized oil-in-water emulsions when mixed with flaxseed gum at neutral pH. *Food Research International, 41*, 964–972.
Klinkesorn, U., Sophanodora, P., Chinachoti, P., Decker, E. A., & McClements, D. J. (2005). Encapsulation of emulsified tuna oil in two-layered interfacial membranes prepared using electrostatic layer-by-layer deposition. *Food Hydrocolloids, 19*, 1044–1053.
Lee, S., Faustman, C., Djordjevic, D., Faraji, H., & Decker, E. A. (2006). Effect of antioxidants on stabilization of meat products fortified with n-3 fatty acids. *Meat Science, 72*(1), 18–24.
Lizarraga, M. S., Pan, L. G., Añón, M. C., & Santiago, L. G. (2008). Stability of concentrated emulsions measured by optical and rheological methods. Effect of processing conditions – I. Whey protein concentrate. *Food Hydrocolloids, 22*, 868–878.
Manoj, P., Fillery-Travis, A. J., Watson, A. D., Hibbered, D. J., & Robins, M. M. (1998). Characterization of a depletion-flocculated polydisperse emulsion: I. Creaming behavior. *Journal of Colloid and Interface Science, 207*, 283–293.
McClements, D. J. (1999). *Food emulsions: Principles, practice, and techniques*. Boca Ratón, Florida, USA: CRC Press.
McClements, D. J. (2000). Comments on viscosity enhancement and depletion flocculation by polysaccharides. *Food Hydrocolloids, 14*, 173–177.
McClements, D. J. (2004). Protein-stabilized emulsions. *Current Opinion in Colloid & Interface Science, 9*, 305–313.
McClements, D. J. (2006). Non-covalent interactions between proteins and polysaccharides. *Biotechnology Advances, 24*, 621–625.
McClements, D. J., & Decker, E. A. (2000). Lipid oxidation in oil-in-water emulsions: impact of molecular environment on chemical reactions in heterogeneous food systems. *Journal of Food Science, 65*(8), 1270–1282.
McClements, D. J., Decker, E. A., & Weiss, J. (2007). Emulsion-based delivery systems for lipophilic bioactive components. *Journal of Food Science, 72*(8), 109–124.
Meller, A., & Stavans, J. (1996). Stability of emulsions with nonadsorbing polymers. *Langmuir, 12*, 301–304.
Molina Ortiz, S. E., Puppo, M. C., & Wagner, J. R. (2004). Relationship between changes and functional properties of soy protein isolates-carrageenan systems. *Food Hydrocolloids, 18*, 1045–1053.
Parker, A., Gunning, P. A., & Robins, M. M. (1995). How does xanthan stabilize salad dressing? *Food Hydrocolloids, 9*, 333–342.
Perrechil, F. A., & Cunha, R. L. (2013). Stabilization of multilayered emulsions by sodium caseinate and κ-carrageenan. *Food Hydrocolloids, 30*, 606–613.
Pongsawatmanit, R., Harnsilawat, T., & McClements, D. J. (2006). Influence of alginate, pH and ultrasound treatment on palm oil-in-water emulsions stabilized by β-lactoglobulin. *Colloids and Surfaces A: Physicochemical and Engineering Aspects, 287*, 59–67.
Radford, S. J., & Dickinson, E. (2004). Depletion flocculation of caseinate-stabilised emulsions: what is the optimum size of the non-adsorbed protein nano-particles? *Colloids and Surfaces A: Physicochemical and Engineering Aspects, 238*, 71–81.
Rodríguez Patino, J. M., & Pilosof, A. M. R. (2011). Protein-polysaccharide interactions at fluid interfaces. *Food Hydrocolloids, 25*, 1925–1937.
Sagalowicz, L., & Leser, M. E. (2010). Delivery for liquid food products. *Current Opinion in Colloid & Interface Science, 15*, 61–72.
Santiago, L. G., Carrara, C. R., & González, R. J. (2005). Interaction of soy protein isolate and meat protein in a model emulsion system. Effect of emulsification order and characteristics of soy isolate used. *Food Science and Technology International, 11*(2), 79–88.
Santiago, L. G., Gonzalez, R. J., Fillery-Travis, A., Robins, M., Bonaldo, A. G., & Carrara, C. (2002). The influence of xanthan and λ-carrageenan on the creaming and flocculation of an oil-in-water emulsion containing soy protein. *Brazilian Journal of Chemical Engineering, 19*(4), 411–417.
Taherian, A. R., Britten, M., Sabik, H., & Fustier, P. (2011). Ability of whey protein isolate and/or fish gelatin to inhibit physical separation and lipid oxidation in fish oil-in-water beverage emulsion. *Food Hydrocolloids, 25*, 868–878.
Uauy, R., & Dangour, A. (2006). Nutrition in brain development and aging: role of essential fatty acids. *Nutrition Reviews, 64*(5), 24–33.
Weinbreck, F. (2004). *Whey protein/gum arabic coacervates: Structure an dynamics* (Thesis). The Netherlands: Ultrech University.